ACS APPLIED MATERIALS & INTERFACES

Research Article

www.acsami.org

Simultaneous Delivery of Multiple Antibacterial Agents from Additively Manufactured Porous Biomaterials to Fully Eradicate Planktonic and Adherent *Staphylococcus aureus*

S. Bakhshandeh,[†,‡] Z. Gorgin Karaji,[†,§] K. Lietaert,[∥,⊥] A. C. Fluit,[#] C. H. E. Boel,[#] H. C. Vogely,[†] T. Vermonden,[¶] W. E. Hennink,[¶] H. Weinans,[†,‡,△] A. A. Zadpoor,[‡] and S. Amin Yavari*[,†,‡]

[†]Department of Orthopedics, [#]Department of Medical Microbiology, and [△]Department of Rheumatology, University Medical Centre Utrecht, 3584 CX Utrecht, The Netherlands

[‡]Department of Biomechanical Engineering, Delft University of Technology, 2628 CD Delft, The Netherlands

[§]Department of Mechanical Engineering, Kermanshah University of Technology, Kermanshah, Iran

[∥]3D Systems - LayerWise NV, 3001 Leuven, Belgium

[⊥]Department of Metallurgy and Materials Engineering, KU Leuven, 3000 Leuven, Belgium

[¶]Department of Pharmaceutics, Utrecht Institute of Pharmaceutical Sciences (UIPS), Utrecht University, 3512 JE Utrecht, The Netherlands

Supporting Information

ABSTRACT: Implant-associated infections are notoriously difficult to treat and may even result in amputation and death. The first few days after surgery are the most critical time to prevent those infections, preferably through full eradication of the micro-organisms entering the body perioperatively. That is particularly important for patients with a compromised immune system such as orthopedic oncology patients, as they are at higher risk for infection and complications. Full eradication of bacteria is, especially in a biofilm, extremely challenging due to the toxicity barrier that prevents delivery of high doses of antibacterial agents. This study aimed to use the potential synergistic effects of multiple antibacterial agents to prevent the use of toxic levels of these agents and achieve full eradication of planktonic and adherent bacteria. Silver ions and vancomycin were therefore simultaneously delivered from additively manufactured highly porous titanium implants with an extremely high surface area incorporating a bactericidal coating made from chitosan and gelatin applied by electrophoretic deposition (EPD). The presence of the chitosan/gelatin (Ch+Gel) coating, Ag, and vancomycin (Vanco) was confirmed by X-ray photoelectron spectroscopy (XPS) and Fourier transform infrared spectroscopy (FTIR). The release of vancomycin and silver ions continued for at least 21 days as measured by inductively coupled plasma (ICP) and UV-spectroscopy. Antibacterial behavior against *Staphylococcus aureus*, both planktonic and in biofilm, was evaluated for up to 21 days. The Ch+Gel coating showed some bactericidal behavior on its own, while the loaded hydrogels (Ch+Gel+Ag and Ch+Gel+Vanco) achieved full eradication of both planktonic and adherent bacteria without causing significant levels of toxicity. Combining silver and vancomycin improved the release profiles of both agents and revealed a synergistic behavior that further increased the bactericidal effects.

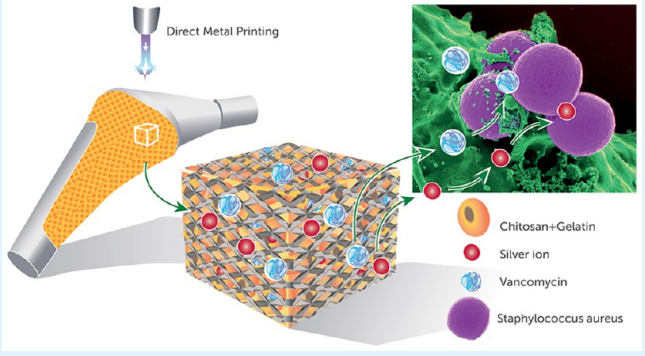

KEYWORDS: *antibacterial surfaces/coatings, porous implants, additive manufacturing, multifunctional biomaterials, hydrogels, electrophoretic deposition*

1. INTRODUCTION

Implant-associated infection (IAI) is one of the major complications in orthopedic and trauma surgery. The infection rates of fracture-fixation, total hip replacement (THR), and total knee replacement (TKR) surgeries are, respectively, around 5%, 1%, and 2%.[1,2] These rates increase exponentially for immunocompromised patients, like patients with (hemato)-oncologic disease or rheumatoid arthritis. After revision surgery infection rates can be as high as 5−40%.[3] IAIs are very difficult and costly to treat and lead to extensive morbidity and even mortality.[4]

To prevent IAI, full eradication of bacteria that enter the body perioperatively is of utmost importance. Local delivery of high doses of antibacterial agents is generally needed to achieve

Received: April 8, 2017
Accepted: July 11, 2017
Published: July 11, 2017

DOI: 10.1021/acsami.7b04950
ACS Appl. Mater. Interfaces 2017, 9, 25691−25699

such full eradication of planktonic and, especially, bacteria in a biofilm.

Local delivery of high doses of antibacterial agents might be achieved through additively manufactured (AM) porous titanium, which has been recently proposed as a promising biomaterial for bone substitution[5,6] as well as for orthopedic implants with improved osseointegration.[7−9] Due to their lower elastic modulus, which is similar to those of bone,[10] porous metallic biomaterials are excellent candidates to prevent stress-shielding. A variety of porous structures with different geometrical designs could be contrived, thereby improving fluid transport, bone tissue regeneration, and, thus, implant fixation.[11−13] More importantly, volume-porous AM structures have an extremely large surface area as compared to nonporous implants.[14,15] The much larger surface area of AM porous biomaterials provides an important advantage, because the intended effects of surface coatings tremendously increase. The surface area could be used for local delivery of high doses of antibacterial agents to achieve a multifunctional biomaterial that combines osteogenic nanotubular surfaces with silver nanoparticles (NPs) that release silver ions and, thus, induce strong antibacterial effects.[16]

The strong antibacterial effects, however, come at the cost of cytotoxicity.[16] The toxic effects are not limited to silver ions, as other antibacterial agents and even antibiotics[17] also show various types of toxicity when administered in high doses needed for full bacterial eradication. Thus, toxicity prevents us from achieving full eradication of planktonic and, especially, bacteria in a biofilm around the implant.

In the current study, we propose to use the potential synergistic effects of multiple antibacterial agents[18,19] to avoid toxicity, but achieve full eradication of bacteria. Silver nanopartiles in combination with vancomycin revealed synergisitic antibacterial effects that make them suitable candidates for this study.[20,21] We therefore applied a coating based on chitosan and gelatin using electrophoretic deposition (EPD) to simultaneously deliver silver ions and vancomycin. Chitosan was chosen because of its bactericidal behavior[22,23] while gelatin was applied for mitigating[24,25] the adverse effects of chitosan on host cells. In the current study, we tested the chemical composition, release profiles, and antibacterial behavior of the materials in both short and long term.

2. MATERIALS AND METHODS

2.1. Materials. Medium molecular weight chitosan (Mw = 300 kDa and 82% degree of deacetylation) and gelatin from porcine skin were purchased from Sigma-Aldrich (Germany). Silver nitrate ($AgNO_3$), vancomycin hydrochloride, and acetic acid (glacial, 99−100%) were also purchased from Sigma-Aldrich (Germany). Chitosan (0.5 mg/mL) and gelatin (1 mg/mL) solutions were obtained by dissolving the respective powders in 1% aqueous acetic acid solution and were subsequently stirred to promote dissolution. All reagents were analytical grade and were used without further purification. All glass containers were washed and rinsed with deionized water.

2.2. Manufacturing. Direct metal printing (DMP) on a ProX DMP 320 machine (3D Systems, Leuven, Belgium) was used to produce volume-porous titanium scaffolds. Magics (Materialise, Leuven, Belgium) and DMP control software were used for file preparation. The specimens had a cylindrical shape with a diameter of 8 mm and a height of 3 mm. The unit cell used had a dodecahedron geometry and a size of 1.1 mm. Pure titanium powder with spherical shape and chemical composition according to ASTM F67 (Grade 1) was used to produce the porous discs that are referred to as the as-manufactured (AsM) specimens from now on (Figure 1). The manufacturing process was executed under inert gas atmosphere with

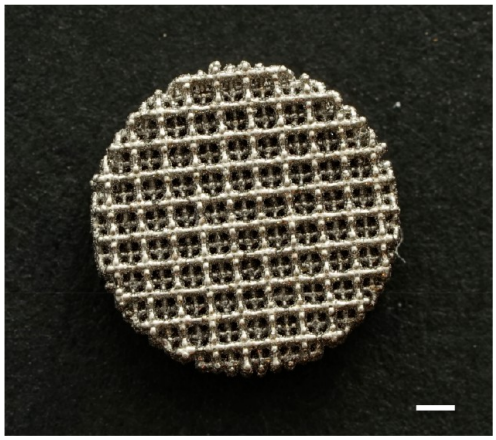

Figure 1. (a) Macrographs of porous titanium specimens (scale bar, 1 mm).

oxygen concentrations below 50 ppm. Afterward, the specimens were cut off the titanium base plate with wire electrical discharge machining and cleaned in demineralized water using ultrasound.

The actual height and diameter of the specimens were measured. The average diameter and height were 8.13 ± 0.02 mm and 3.15 ± 0.03 mm, respectively. Based on these values, the relative density was calculated as 37.19 ± 0.83%. To assess the density of the bulk material of the struts, an OHAUS Pioneer PA214C balance and a density kit were used. Based on the Archimedes technique, the average strut (i.e., matrix material) density of 10 samples was 98.78 ± 0.63%.

2.3. Electrophoretic Deposition (EPD). A platinum mesh was chosen as the anode, while the porous titanium specimens, placed at 1 cm distance, was the cathode. The deposition time (60 s to 20 min) and applied voltage (3.5−20 V) were optimized through a parametric study. Relatively homogeneous film was achieved with 10 V applied over 5 min of deposition. At the end of the process, the coated specimens were gently removed, rinsed with Milli-Q water, and left to dry at room temperature overnight. The unloaded chitosan and gelatin coating is referred to as 'Ch+Gel'. To incorporate vancomycin and silver into the coating, 0.5 mg/mL vancomycin (Ch+Gel+Vanco group) or silver nitrate (1 mM) (Ch+Gel+Ag group) solutions were mixed with the chitosan/gelatin compound for 45 min before deposition. For simultaneous delivery of both silver ions and vancomycin, lower concentrations of vancomycin, i.e., 0.2 mg/mL, was combined with silver nitrate (1 mM) (Ch+Gel+Ag+Vanco group).

2.4. Surface Characterization. The optical photographs of the coatings were taken immediately after EPD with a Keyence (VH-Z20R/W/T, USA) microscope. Moreover, to assess whether the polymer had reached the inner parts of the scaffold, cross-section pictures were taken. For microscale pictures, a JEOL (JSM-6500F, Tokyo, Japan) scanning electron microscope (SEM) was used for observing the surface morphology. To estimate the thickness of the coating, a diamond tip was used to scratch the surface, followed by tilting the samples to 59.4°. In addition, the stability of the coating was assessed by comparing freshly coated samples with specimens left in sterile phosphate-buffered saline (PBS) for up to 28 days. Subsequently, they were analyzed using electron microscopy, comparing their structure and thickness with fresh specimens. The chemical compositions on the surface of the specimens were determined using both X-ray photoelectron spectroscopy (XPS) and Fourier's transform infrared spectroscopy (FTIR). The XPS analysis was performed using an Al Kα X-ray source with 1486.6 eV energy (K-AlphaTM, Thermo Electron, USA). For characterizing all binding energies, the reference peak was that of the C 1s (at 284.84 eV). The atomic percentage of all elements was obtained by normalizing the area of their corresponding peak with respect to the sum of the peaks of all elements. For the FTIR analysis, a PerkinElmer Spotlight (Waltham, Massachusetts, US) machine equipped with a mercury

DOI: 10.1021/acsami.7b04950
ACS Appl. Mater. Interfaces 2017, 9, 25691−25699

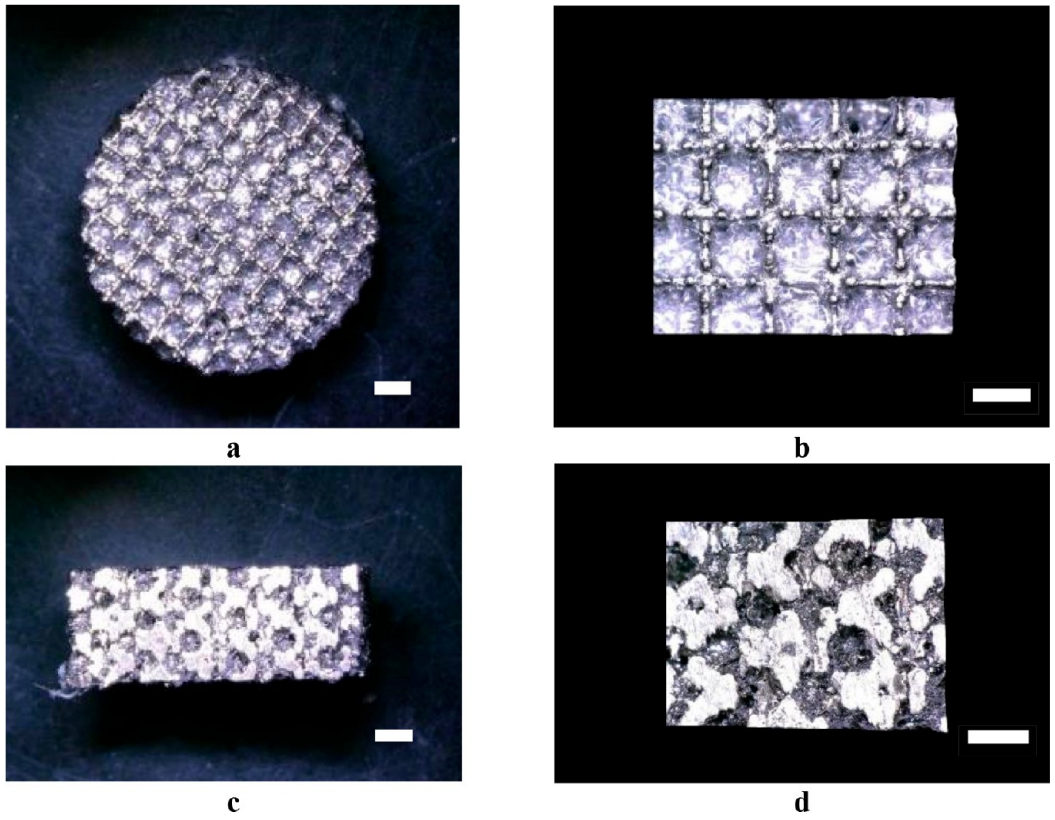

Figure 2. Optical microscopy image of the coated porous titanium: (a) 5×, (b) 100×. The cross section of a coated specimen. EPD enables application of hydrogels as a filler as well as a coating: (c) 5×, (d) 100× (scale bar, 1 mm).

cadmium telluride (MCT) detector was employed. The scanning parameters were as follows: resolution, 2 cm^{-1}; number of scans per spectrum, 32; and wavenumber range, 3200−750 cm^{-1}.

2.5. Ag^+ Release. Inductively coupled plasma mass spectroscopy (ICP-MS, Spectro Arcos) was used to measure the release of silver ions in the Ch+Gel+Ag and Ch+Gel+Ag+Vanco groups. Three samples per group were immersed in 500 μL of Milli-Q water and kept in an incubator at 37 ± 0.5 °C. The measurements were performed for time points 6 h, and 1, 3, 7, 14, and 21 days. The medium was refreshed completely after each time point. The measurements were repeated three times.

2.6. Vancomycin Release. UV−vis spectroscopy (Spectrostar Nano, BMG Labtech, Germany) was used to measure the vancomycin release at time points 6 h, and 1, 3, 7, 14, and 21 days. For each of the experimental groups, three samples per time point were kept in a phosphate-buffered saline solution (PBS) at 37 ± 0.5 °C and the medium was refreshed completely after each time point. The wavelength of the measurements was 280 nm. Each test was repeated three times to ensure the reproducibility of the results. A calibration curve with a root-mean-square (R^2) of ≥0.998 was established by using different vancomycin solutions with concentrations of 1−100 μg/mL in PBS.

2.7. Minimum Inhibitory Concentration (MIC) of Silver and Vancomycin against *S. aureus*. A *S. aureus* strain (ATCC 6538) was grown overnight on blood agar plates at 37 °C. It was subsequently passed from the plate to 4 mL Cation Adjusted Mueller Hinton (CAMH) broth and incubated at 37 °C overnight. A fresh bacterial suspension was then prepared by adding 100 μL of the overnight culture to 4 mL fresh CAMH broth and incubated for approximately 2.5 h at 37 °C until OD: 0.6. This was diluted in 3× CAMH broth to OD: 0.06−0.01.

Next, 65 μL samples of the dilutions were transferred into a fresh tube with 10 mL CAMH broth. Then, a 2-fold dilution series of vancomycin was made in Milli Q in a 96-well plate.

For the combination of vancomycin and silver, 50 μL bacterial suspension, 50 μL vancomycin, and 50 μL silver nitrate were mixed.

2.8. Antibacterial Assay. *S. aureus* ATCC 6538 strain was used as a model pathogen to assess both the short-term (6 h, 1 and 3 days) and long-term (7, 14, and 21 days) antimicrobial potential of the different experimental groups. A TSB medium supplemented with 1% glucose was used to culture the bacteria at 37 °C for 18 h. After dilution to OD600 0.01, the bacterial suspension was seeded on the specimens (three specimens per group for each time point) and incubated at 37 °C. For the long-term, planktonic antimicrobial efficiency was assessed, while for short-term, due to the possible presence of adherent bacteria or biofilm, both planktonic and adherent antimicrobial efficiencies were determined. The method adopted to enumerate planktonic and adherent bacteria was the plate counting method using serial dilution. To quantitatively assess adherent (biofilm) bacteria, the specimens were first rinsed with PBS three times, vortexed for 30 s in 2 mL PBS, and shaken for 15 min to remove the nonadherent bacteria.

2.9. Cell Culture and Live/Dead Assay. Osteoblast-like cells (2 × 10^5 cells per specimen) from cell line MG-63 (ATCC, Germany) were cultured on three specimens from every experimental group. The culture medium was α-MEM medium (Invitrogen, USA) supplemented with 1% antibiotics (penicillin/streptomycin, Invitrogen, USA), 10% fetal bovine serum (Cambrex, US), and 0.2 mM L-ascorbic acid-2-phosphate (AsAP, Sigma-Aldrich, Germany) incubated at 37 °C, 5% CO_2. Live/dead staining was performed after 2 days. The samples were incubated at 37 °C for 30 min in fresh medium containing 2 μM calcein AM and 8 μM ethidium homodimer-1 (Life Technologies, UK) as the staining medium. A fluorescence microscope (Olympus BX51, Japan) was used to qualitatively assess live (stained green) and dead (stained red) cells.

For quantitative metabolic activity, the resazurin (Alamar Blue) assay was employed at 1 and 3 days after culture. Alamar blue solution was prepared by dissolving 440 mM of resazurin (resazurin sodium salt, Sigma-Aldrich, Germany) in PBS, followed by a 10% dilution by

DOI: 10.1021/acsami.7b04950
ACS Appl. Mater. Interfaces 2017, 9, 25691−25699

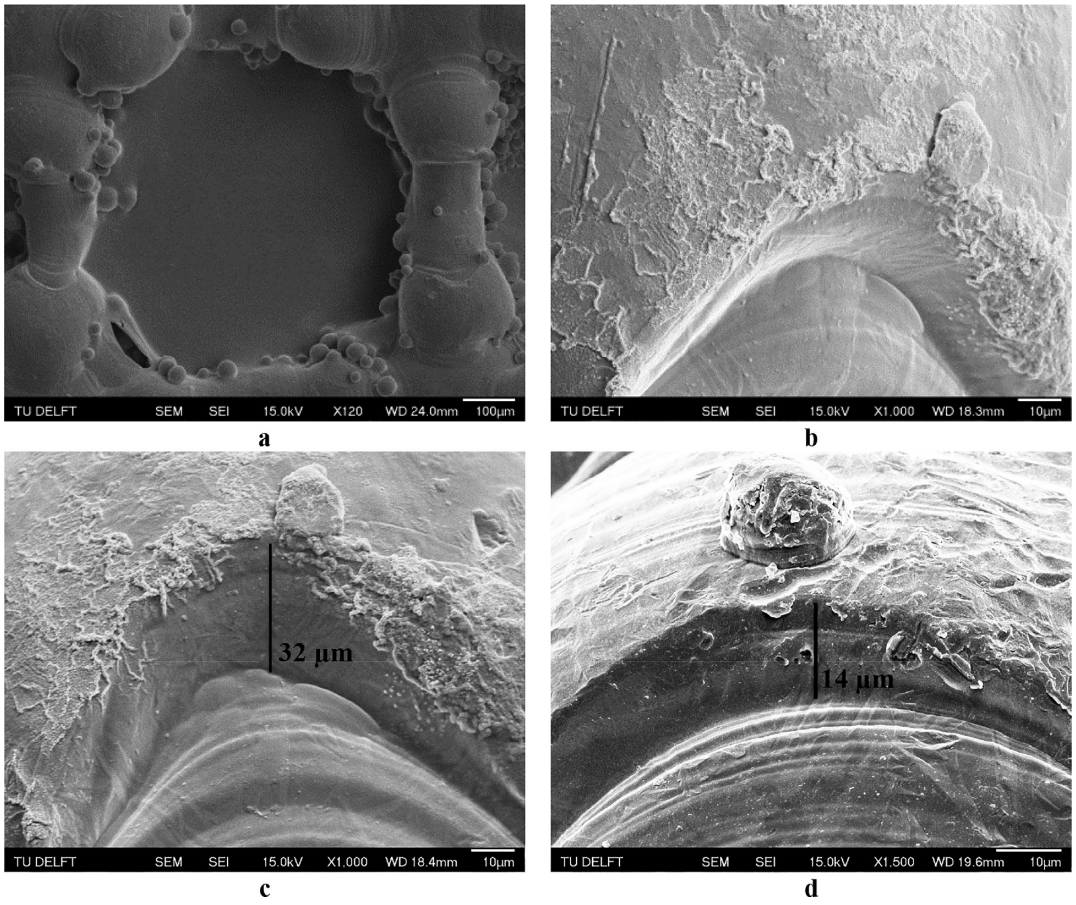

Figure 3. SEM pictures of the coated specimens show successful deposition of the polymer: (a) 120×, (b) 1000×. A selected spot at which the coated and noncoated parts of the specimen could be concurrently seen in order to estimate the coating thickness: (c) fresh coating (1000×); (d) after 28 days (1500×).

adding the α-MEM medium (Invitrogen, US) supplemented with FBS (10%) (Cambrex, US) for a total of 600 μL per sample (three per group). The absorbance was measured at 544 nm (570 nm of subtraction) with a microplate reader (Fluoroskan Ascent FL, Thermo Fisher Scientific, Spain).

2.10. Statistical Analysis. One-way ANOVA with Tukey-Kramer posthoc analysis was performed with MATLAB R2016b (Mathworks, Natik, MA, USA) to assess the statistical significance of the differences found between experimental groups (threshold 0.05).

3. RESULTS

The nanocomposite coating achieved with EPD resulted in a relatively uniform film composed of chitosan and gelatin covering the surface of the implant as well as the inner struts, optimally exploiting the high surface area of volume-porous specimens (Figure 2a,b). The polymers deposited through EPD reached some of the inner parts of the porous structure (Figure 2c,d). The internal surfaces of the specimens were covered with uniform Ch-Gel coating (Figure 3a,b) with an average thickness of around 32 μm (Figure 3c) which reduced to 14 μm (Figure 3d), i.e., nearly half of the fresh ones, after 28 days immersion in PBS with clear signs of degradation. The ATR-FTIR spectrum of chitosan−gelatin matrix, showed strong peaks at 1100, 1150, 1300, 1630, and 1550 cm^{-1} (Figure 4). The first three values are distinctive of polysaccharide structures for C−N stretching, C−O stretching, and O−H bending, respectively.[26] On the other hand, 1630 and 1550 cm^{-1} are spectrum peaks characteristic of gelatin, due to amide I, −CONH−

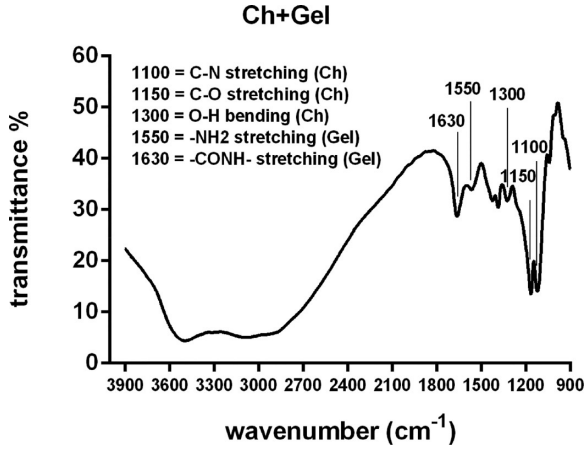

Figure 4. FTIR spectra of chitosan and gelatin polymeric matrix.

stretching, and amide II, $-NH_2$ stretching, respectively. The surface elemental composition results (Figure 5) showed double-peaks at 464 and 458 eV, which are, respectively, representative of Ti $2p_{1/2}$ and Ti $2p_{3/2}$, validating the composition of the titanium bulk material. The high amounts of carbon and nitrogen confirm the presence of chitosan and gelatin. High resolution XPS has been performed to assess in detail the orbital splitting of silver (Figure 5f). The Ag $3d_{5/2}$ peak could be split into two subpeaks after deconvolution: one at 367.9 eV and one at 368.4 eV, revealing the contribution of

DOI: 10.1021/acsami.7b04950
ACS Appl. Mater. Interfaces 2017, 9, 25691−25699

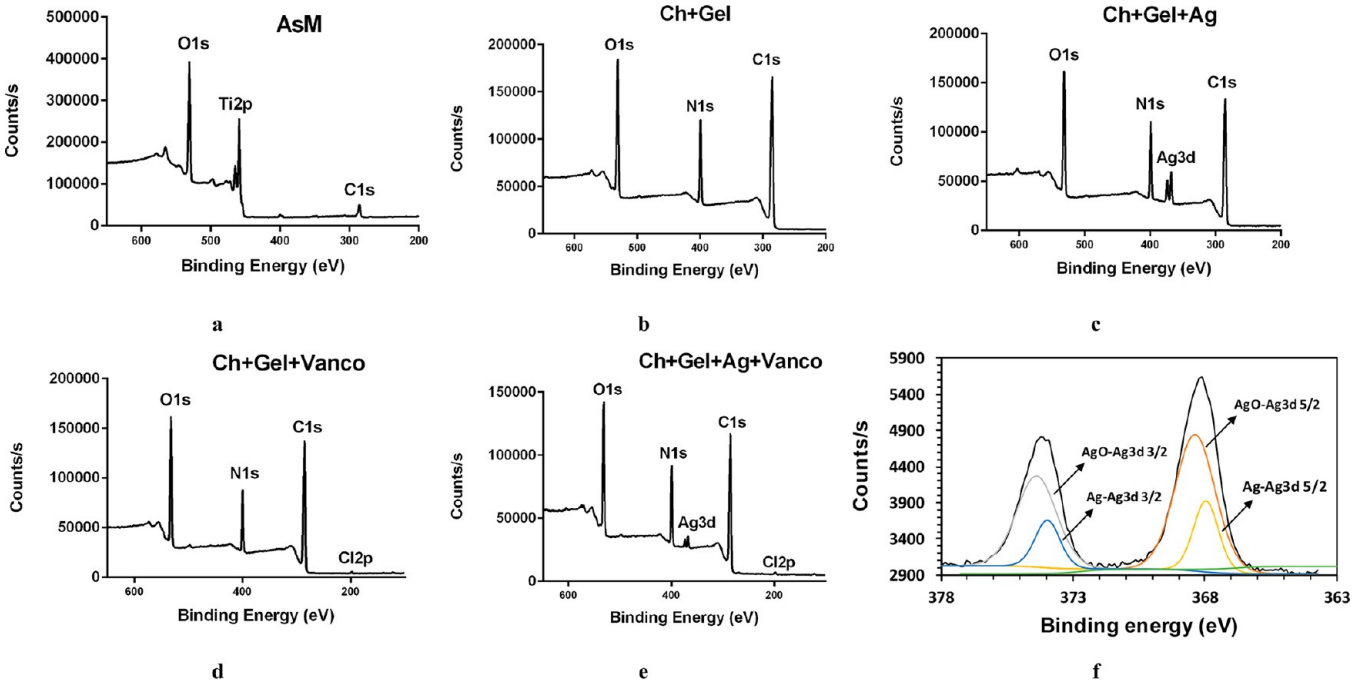

Figure 5. XPS spectra of the specimens from (a) AsM, (b) Ch+Gel, (c) Ch+Gel+Ag, (d) Ch+Gel+Vanco, (e) Ch+Gel+Ag+Vanco groups, and (f) high resolution spectra of silver.

both Ag and its oxides, more specifically AgO.[27] Ag $3d_{3/2}$ is also composed of two peaks at 372.9 and 374.4 eV, again corresponding to the presence of both Ag and its oxide compounds.[28] These results are line with those found in previous studies.[29,30] The peak at 200 eV affirms the presence of Cl, which is representative of vancomycin. The slightly high concentration of C could be assigned to imide and amide groups.[31] All the characteristic peaks seen in the previous pictures are observed in the combination group as well, validating the presence of both antimicrobial agents.

The MIC values of vancomycin and silver ions ($AgNO_3$) were 0.5 μg/mL and 97.7 μM (8.3 ppm), respectively (Figure S1). More than 1 order of magnitude lower concentration of silver ions (corresponding to a drop in $AgNO_3$ concentration from 48.8 to 3.1 μM) was needed when 0.25 μg/mL of vancomycin was present.

As for the release of vancomycin from Ch+Gel+Vanco and Ch+Gel+Vanco+Ag groups, the former group showed an initial burst release, followed by a slow release down to 0.7 μg/mL after 21 days (Figure 6a). The combination group, on the other hand, showed a much slower release such that at time points 14 and 21 days it even surpassed the Ch+Gel+Vanco concentrations (Figure 6a).

After an initial burst release, the concentration of silver ions had already fallen below the MIC at day 1 for Ch+Gel+Ag (Figure 6b). The combination group, on the other hand, showed a substantially slower release with no sign of burst release, which is in line with the release profile of vancomycin for Ch+Gel+Ag+Vanco (Figure 6a). Nonetheless, the values of silver ions released for this group were all below the MIC from the first time point on.

A very low level of toxicity was detected for Ch+Gel at day 1 but not at day 3 (Figure 7). Cytotoxicity was observed for silver-containing groups at both time points, nonetheless, cell proliferation was noticed at day 3 as compared to day 1 (Figure 7). The coating containing only vancomycin showed no toxicity

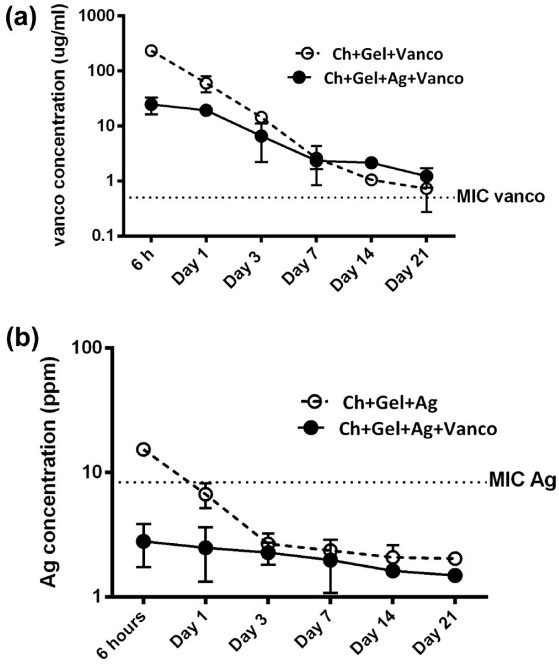

Figure 6. Release profile of vancomycin (a) and silver ions (b) from the different groups and comparison with the MIC line.

(Figure 7). According to the live/dead assay (Figure 8), except for the groups containing silver, no other group showed cytotoxic effects, which is in line with the results of the Alamar blue assay. Although the presence of dead cells (red dots) is noticeable in two groups, some proliferation could still be observed after 2 days (Figure 8).

As compared to the AsM group, the Ch+Gel (containing only chitosan and gelatin) group showed over 2 log reduction in the number of the planktonic and biofilm bacteria for up to 24 h (Figure 9 a,c). This efficiency dropped dramatically for

DOI: 10.1021/acsami.7b04950
ACS Appl. Mater. Interfaces 2017, 9, 25691−25699

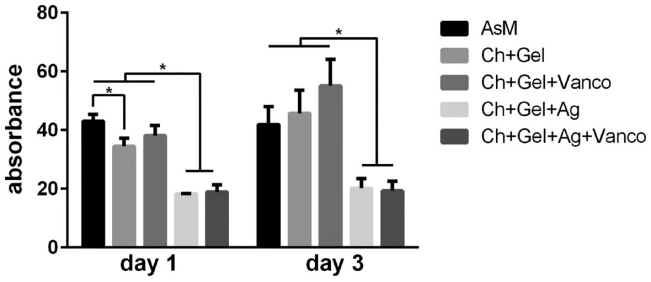

Figure 7. Alamar blue assay results for the specimens from different groups for up to 7 days.

planktonic bacteria at day 3 and the subsequent long-term time points (Figure 9a,b), while for the adherent bacteria a nearly 75% effectiveness was still retained at day 3 (Figure 9c). No bacterial inhibition was seen after 7 days for the Ch+Gel group (Figure 9b). All the other agent-containing groups maintained at least 5 log reduction of both planktonic and biofilm bacteria up to the last time point, i.e., 21 days.

4. DISCUSSION

Here we showed that simultaneous delivery of silver ions and vancomycin from additively manufactured porous biomaterials together with the antibacterial effects of chitosan could be used to fully eradicate planktonic and adherent bacteria with only moderate levels of cytotoxicity for the host cells. According to the Gristina's concept of "race for the surface",[32] if host cells and proteins reach the implant before bacteria, there is a high chance that they will cover it, thereby preventing colonization by pathogens. There is, however, a toxicity barrier that often prevents full eradication with a single antibacterial agent without causing a high level of toxicity. While eradication of planktonic bacteria should be possible with concentrations somewhat higher than MIC, much higher concentrations of antibacterial agents may be needed to fully eradicate adherent bacteria, and up to 1000 times higher concentrations have been reported to kill adherent (biofilm-related) bacteria.[33] This could have serious toxicity concerns for silver ions[16,34] as well as vancomycin that might cause nephrotoxicity.[35] With the current designs of chitosan−gelatin EPD-based delivery system, full eradication for both planktonic and adherent bacteria is reached with Ag, vancomycin, and their combination.

The delivery system itself has some bactericidal activity likely through the collapse of the bacterial membrane[22] caused by interaction of the negatively charged teichoic acid's phosphate groups present in the *S. aureus* membrane with the positively charged amine groups of chitosan.

This contact-killing approach could also negatively affect host cell adhesion and impart implant integration. However, the second component of the delivery system, i.e., gelatin, presents RGD motifs, which prompt adhesion of osteoblasts that likely compensates the toxicity of chitosan (Figures 7, 8). At day 1, a statistically significant difference is seen between AsM and Ch+Gel groups in the Alamar blue assay, which might exhort a potential toxic effect of chitosan. According to the FDA-approved ISO 10993−5 standard for quantitative biological evaluation of medical devices, "a reduction of cell viability by more than 30% is considered a cytotoxic effect".[36] However, the difference between AsM and Ch+Gel at day 1 is less than 11%, meaning that the observed levels of cytotoxicity have limited practical relevance.

When adding silver to the Ch+Gel, the specimens achieved full eradication of both planktonic and adherent bacteria, while only moderate levels of cytotoxicity were observed. Given that the concentration of silver ions is rather low, this effect is likely

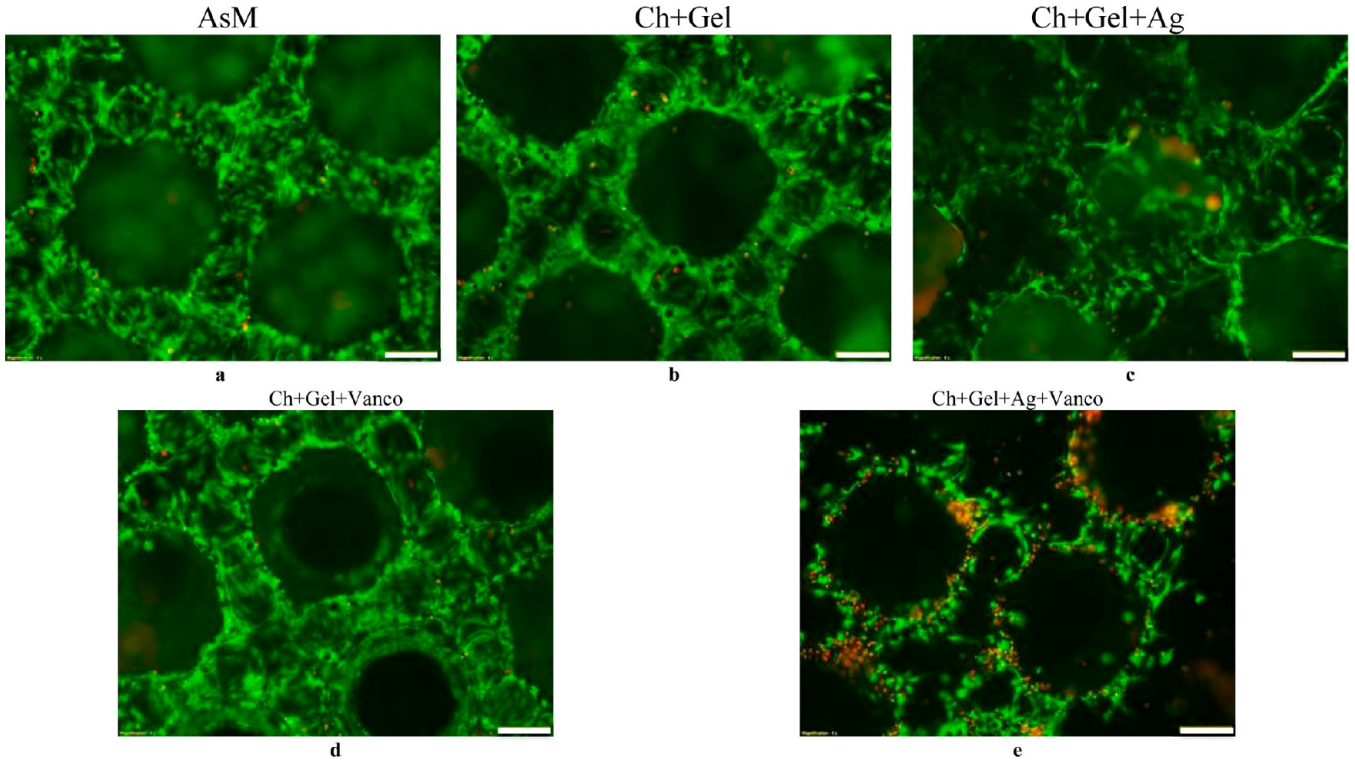

Figure 8. Live/dead images on MG63 osteoblast cells for all the experimental groups after 2 days (scale bar 200 μm): (a) AsM, (b) Ch+Gel, (c) Ch+Gel+Ag, (d) Ch+Gel+Vanco, (e) Ch+Gel+Ag+Vanco.

DOI: 10.1021/acsami.7b04950
ACS Appl. Mater. Interfaces 2017, 9, 25691−25699

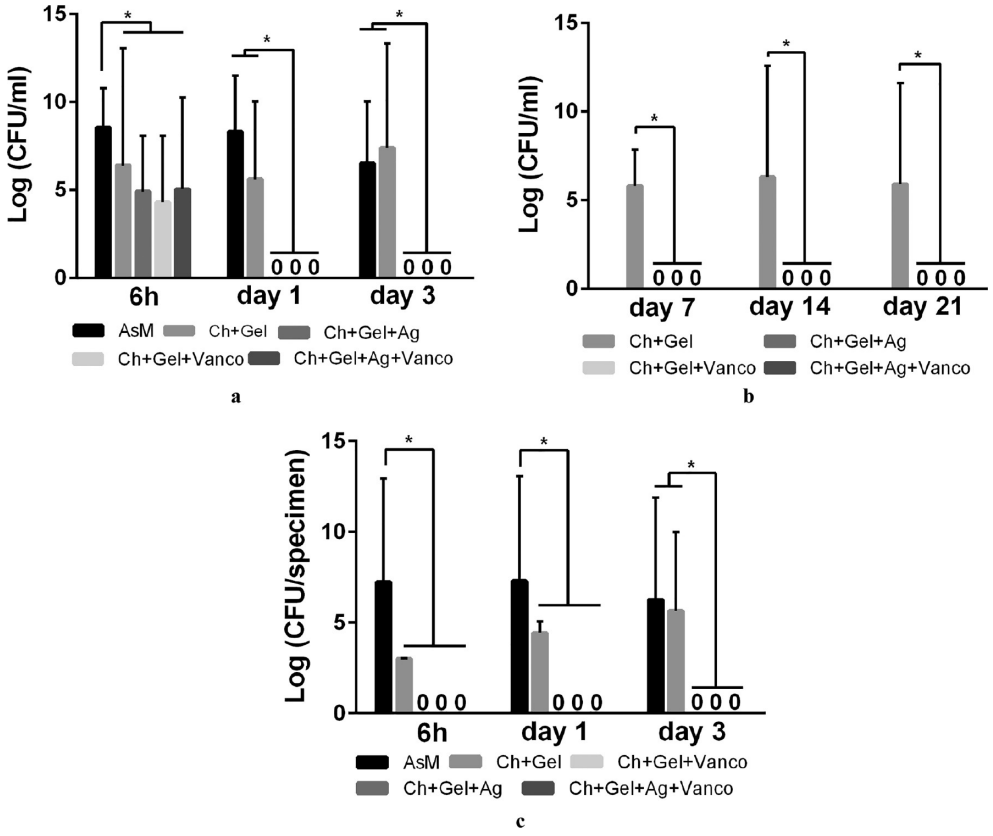

Figure 9. Short-term (a) and long-term (b) killing effect against planktonic bacteria as well as the short-term killing effect against adherent bacteria (c).

attributed to the synergy between silver ions and chitosan, as reported earlier.[37−39] As a consequence, the cytotoxicity level is limited as compared to the designs we presented in a previous study.[16] Since silver is active against a broad spectrum of bacteria[40] including methicillin-resistant *Staphylococcus aureus* (MRSA), this potential solution for the cytotoxicity problem could open new avenues for its safe clinical application.

From a mechanistic viewpoint, the antimicrobial mechanism of silver is conceived to consist of contact-killing by means of positive ions that permeabilize bacterial membranes by interacting with its thiol groups, causing DNA condensation, and impairing growth.[41] The presence of chitosan as our main polymeric matrix, with its amino and hydroxyl ligands that could act as anchoring sites for metal ions may (absorb and therefore) reduce the amount of silver ions released in the environment.[42] As chitosan increases the permeability of the bacterial membrane, the silver ions will more easily enter and kill the bacteria.[38] A number of additional action mechanisms[37,39] including the effects of the positive charges of chitosan on improving the binding of silver to the anionic bacterial membrane have been also suggested.

The specimens with the Ch+Gel+Vanco group also achieved full eradication of bacteria while not exhibiting any sign of cytotoxicity. However, the release profile of vancomycin shows that the concentration of vancomycin at 6 h, 1 day, and 3 days is, respectively, 460, 120, and 28 times higher than the MIC. While such high systemic levels of vancomycin could normally lead to nephrotoxicity levels,[35] the current concentrations are only local and systematic concentrations will be much lower away from the implant, likely being substantially lower, depending on the implant size and amount of coating applied.

Adding silver to the previously discussed group of Ch+Gel +Vanco again fully eradicated both planktonic and adherent bacteria but induced some level of cytotoxicity for the MG-63 cells similar to the Ch+Gel+Ag group. An interesting observation was that the addition of silver tremendously decreases the burst release of vancomycin during the first few hours to first few days (Figure 6a), making the vancomycin levels considerably lower, likely further lowering chances of nephrotoxicity particularly for larger implants. A similar effect was observed for silver ions (Figure 6b), which was reduced by a factor of 5 at 6 h as compared to the Ch+Gel+Ag. Even though the concentrations of both agents are much lower, the specimens from this group with combined agents apparently behave in a synergistic manner[43] showing extremely high levels of bactericidal effects and achieving full eradication of planktonic bacteria while inhibiting biofilm formation. From the mechanistic viewpoint, the increased membrane permeability due to the presence of silver ions (even at sublethal concentrations) has been proposed as a boosting mechanism for the activity of larger antibiotics like vancomycin against both Gram-positive and Gram-negative bacteria.[18,19,43]

4.1. Clinical Perspective. Complex bone reconstruction as well as trauma and implant revision surgeries often necessitate large wounds that are open for several hours with a significant chance that a sizable number of bacteria will enter the body and induce an infection during the first days when the implant is not encapsulated by host cells. Failure to fully eradicate those bacteria could result in biofilm formation that is notoriously difficult to treat.[44,45] In particular, the immune systems of the most vulnerable patients such as orthopedic oncologic or rheumatoid patients may be too compromised to handle the

DOI: 10.1021/acsami.7b04950
ACS Appl. Mater. Interfaces 2017, 9, 25691−25699

perioperative influx of bacteria. The results of the current study show that simultaneous delivery of multiple antibacterial agents is a promising approach to achieve full eradication of bacteria, while addressing the local and systemic toxicity concerns.

Not only can the simultaneous delivery of silver and vancomycin exploit the synergistic antibacterial effects, but it could also offer advantages in terms of adjusting the burst release from a few hours to a few days, thus preserving the drug reservoir for more sustained delivery as well as mitigating some (short-term) toxicity concerns. Due to the open pore space with huge surface area, the porous implant with an electrophoretic deposition based coating enables controlled (high dose) release of multiple antibacterial agents as well as growth factors.[46] Chemotherapy and/or radiotherapy treatments experienced by the orthopedic oncologic patients not only compromises the immune system but could also impair bone metabolism,[47−49] thereby lowering bone quality and making osseointegration and implant fixation more challenging. Further optimization with additional delivery of drugs and growth factors to stimulate osseointegration could therefore be of high clinical relevance.

5. CONCLUSIONS

In this study, we covered the huge surface area of additively manufactured porous biomaterials with electrophoretic deposition based coatings made from chitosan and gelatin that release silver ions and vancomycin. Compared to the previous studies with silver, where huge levels of cytotoxicity were required to achieve strong bactericidal effects, the results of the current study show how simultaneous delivery of silver and vancomycin achieves full eradication of bacteria and acceptable levels of toxicity for osteoblast (host) cells. This delivery method of multiple bactericidal compounds in combination with highly porous implants can greatly improve infection therapy in trauma and orthopedic surgery.

■ ASSOCIATED CONTENT

Supporting Information

The Supporting Information is available free of charge on the ACS Publications website at DOI: 10.1021/acsami.7b04950.

Table of MIC results for vancomycin, $AgNO_3$, and their combination against *S. aureus*. Agar plates used for CFU counting after 1 day. The first (a to e) and second (f to j) rows correspond to planktonic and adherent bacteria, respectively. (PDF)

■ AUTHOR INFORMATION

Corresponding Author

*E-mail: s.aminyavari@umcutrecht.nl, saber.aminyavari@gmail.com. Tel: +31-88-7559025.

ORCID

S. Bakhshandeh: 0000-0001-6956-7900
Z. Gorgin Karaji: 0000-0003-2719-7192
T. Vermonden: 0000-0002-6047-5900
H. Weinans: 0000-0002-2275-6170
S. Amin Yavari: 0000-0003-1677-5751

Author Contributions

S.A. conceived the project and designed the study. S.B. carried out the experiments and characterizations. Z.G. conducted the cytotoxicity experiments. K.L. designed and printed the implants. A.F. and E.B. conducted the antibacterial tests and analysis. T.V., W.H., H.V., H.W., A.Z., and S.A. discussed and interpreted the results. S.B., A.Z., and S.A. wrote the manuscript.

Notes

The authors declare no competing financial interest.

■ ACKNOWLEDGMENTS

This work was supported by the PROSPEROS project from Interreg program and also was partially supported by funding of the agency for Innovation by Science and Technology (IWT) of the Flemish government through Baekeland mandate "IWT140257".

■ REFERENCES

(1) Edwards, J. R.; Peterson, K. D.; Mu, Y.; Banerjee, S.; Allen-Bridson, K.; Morrell, G.; Dudeck, M. A.; Pollock, D. A.; Horan, T. C. National Healthcare Safety Network (NHSN) report: Data summary for 2006 through 2008, issued December 2009. *Am. J. Infect. Control* **2009**, *37* (10), 783−805.

(2) Zimmerli, W.; Trampuz, A.; Ochsner, P. E. Prosthetic-Joint Infections. *N. Engl. J. Med.* **2004**, *351* (16), 1645−1654.

(3) Widmer, A. F. New Developments in Diagnosis and Treatment of Infection in Orthopedic Implants. *Clin. Infect. Dis.* **2001**, *33*, S94−S106.

(4) Steckelberg, J. M.; Osmon, D. R. Prosthetic Joint Infections. In *Infections Associated with Indwelling Medical Devices*, 3rd ed.; American Society of Microbiology, 2000.

(5) van der Stok, J.; Koolen, M.; de Maat, M.; Yavari, S. A.; Alblas, J.; Patka, P.; Verhaar, J.; van Lieshout, E.; Zadpoor, A. A.; Weinans, H. Full Regeneration of Segmental Bone Defects using Porous Titanium Implants Loaded with BMP-2 Containing Fibrin Gels. *Eur. Cells Mater.* **2015**, *29*, 141−154.

(6) Van der Stok, J.; Van der Jagt, O. P.; Amin Yavari, S.; De Haas, M. F.; Waarsing, J. H.; Jahr, H.; Van Lieshout, E. M.; Patka, P.; Verhaar, J. A.; Zadpoor, A. A. Selective Laser Melting-Produced Porous Titanium Scaffolds Regenerate Bone in Critical Size Cortical Bone Defects. *J. Orthop. Res.* **2013**, *31* (5), 792−799.

(7) Fukuda, A.; Takemoto, M.; Saito, T.; Fujibayashi, S.; Neo, M.; Pattanayak, D. K.; Matsushita, T.; Sasaki, K.; Nishida, N.; Kokubo, T.; Nakamura, T. Osteoinduction of Porous Ti Implants with a Channel Structure Fabricated by Selective Laser Melting. *Acta Biomater.* **2011**, *7* (5), 2327−2336.

(8) van der Stok, J.; Wang, H.; Amin Yavari, S.; Siebelt, M.; Sandker, M.; Waarsing, J. H.; Verhaar, J. A.; Jahr, H.; Zadpoor, A. A.; Leeuwenburgh, S. C. Enhanced Bone Regeneration of Cortical Segmental Bone Defects using Porous Titanium Scaffolds Incorporated with Colloidal Gelatin Gels for Time-And Dose-Controlled Delivery of Dual Growth Factors. *Tissue Eng., Part A* **2013**, *19* (23−24), 2605−2614.

(9) Jiang, Q.-H.; Liu, L.; Peel, S.; Yang, G.-L.; Zhao, S.-F.; He, F.-M. Bone Response to the Multilayer BMP-2 Gene Coated Porous Titanium Implant Surface. *Clin Oral Implants Res.* **2013**, *24* (8), 853−861.

(10) Ahmadi, S. M.; Yavari, S. A.; Wauthle, R.; Pouran, B.; Schrooten, J.; Weinans, H.; Zadpoor, A. A. Additively Manufactured Open-Cell Porous Biomaterials Made from Six Different Space-Filling Unit Cells: fhe Mechanical fnd Morphological Properties. *Materials* **2015**, *8* (4), 1871−1896.

(11) Gibson, L. J.; Ashby, M. F. *Cellular Solids: Structure and Properties*; Cambridge University Press, 1999.

(12) Wen, C. E.; Mabuchi, M.; Yamada, Y.; Shimojima, K.; Chino, Y.; Asahina, T. Processing of Biocompatible Porous Ti and Mg. *Scr. Mater.* **2001**, *45* (10), 1147−1153.

(13) Ryan, G.; Pandit, A.; Apatsidis, D. P. Fabrication Methods of Porous Metals for use in Orthopaedic Applications. *Biomaterials* **2006**, *27* (13), 2651−2670.

DOI: 10.1021/acsami.7b04950
ACS Appl. Mater. Interfaces 2017, 9, 25691−25699

(14) Yavari, S. A.; van der Stok, J.; Chai, Y. C.; Wauthle, R.; Birgani, Z. T.; Habibovic, P.; Mulier, M.; Schrooten, J.; Weinans, H.; Zadpoor, A. A. Bone Regeneration Performance of Surface-Treated Porous Titanium. *Biomaterials* **2014**, *35* (24), 6172−6181.
(15) van Hengel, I. A. J.; Riool, M.; Fratila-Apachitei, L. E.; Witte-Bouma, J.; Farrell, E.; Zadpoor, A. A.; Zaat, S. A. J.; Apachitei, I. Selective Laser Melting Porous Metallic Implants with Immobilized Silver Nanoparticles Kill and Prevent Biofilm Formation by Methicillin-Resistant Staphylococcus aureus. *Biomaterials* **2017**, *140*, 1−15.
(16) Amin Yavari, S.; Loozen, L.; Paganelli, F. L.; Bakhshandeh, S.; Lietaert, K.; Groot, J. A.; Fluit, A. C.; Boel, C. E.; Alblas, J.; Vogely, H. C. Antibacterial Behavior of Additively Manufactured Porous Titanium with Nanotubular Surfaces Releasing Silver Ions. *ACS Appl. Mater. Interfaces* **2016**, *8* (27), 17080−17089.
(17) van Hal, S. J.; Paterson, D. L.; Lodise, T. P. Systematic Review and Meta-Analysis of Vancomycin-Induced Nephrotoxicity Associated with Dosing Schedules That Maintain Troughs between 15 and 20 mg per Liter. *Antimicrob. Agents Chemother.* **2013**, *57* (2), 734−744.
(18) Naqvi, S. Z. H.; Kiran, U.; Ali, M. I.; Jamal, A.; Hameed, A.; Ahmed, S.; Ali, N. Combined Efficacy of Biologically Synthesized Silver Nanoparticles and Different Antibiotics Against Multidrug-Resistant Bacteria. *Int. J. Nanomed.* **2013**, *8*, 3187−3195.
(19) Shahverdi, A. R.; Fakhimi, A.; Shahverdi, H. R.; Minaian, S. Synthesis and Effect of Silver Nanoparticles on the Antibacterial Activity of Different Antibiotics Against Staphylococcus aureus and Escherichia coli. *Nanomedicine* **2007**, *3* (2), 168−171.
(20) Varisco, M.; Khanna, N.; Brunetto, P. S.; Fromm, K. M. New Antimicrobial and Biocompatible Implant Coating with Synergic Silver−Vancomycin Conjugate Action. *ChemMedChem* **2014**, *9* (6), 1221−1230.
(21) Okano, A.; James, R. C.; Pierce, J. G.; Xie, J.; Boger, D. L. Silver(I)-Promoted Conversion of Thioamides to Amidines: Divergent Synthesis of a Key Series of Vancomycin Aglycon Residue 4 Amidines That Clarify Binding Behavior to Model Ligands. *J. Am. Chem. Soc.* **2012**, *134* (21), 8790−8793.
(22) Junter, G.-A.; Thébault, P.; Lebrun, L. Polysaccharide-Based Antibiofilm Surfaces. *Acta Biomater.* **2016**, *30*, 13−25.
(23) Raafat, D.; Sahl, H.-G. Chitosan and its Antimicrobial Potential − A Critical Literature Survey. *Microb. Biotechnol.* **2009**, *2* (2), 186−201.
(24) Jiankang, H.; Dichen, L.; Yaxiong, L.; Bo, Y.; Hanxiang, Z.; Qin, L.; Bingheng, L.; Yi, L. Preparation of Chitosan−Gelatin Hybrid Scaffolds with Well-Organized Microstructures for Hepatic Tissue Engineering. *Acta Biomater.* **2009**, *5* (1), 453−461.
(25) Shi, Z.; Neoh, K. G.; Kang, E. T.; Poh, C.; Wang, W. Bacterial Adhesion and Osteoblast Function on Titanium with Surface-Grafted Chitosan and Immobilized RGD Peptide. *J. Biomed. Mater. Res., Part A* **2008**, *86A* (4), 865−872.
(26) Jiang, T.; Zhang, Z.; Zhou, Y.; Liu, Y.; Wang, Z.; Tong, H.; Shen, X.; Wang, Y. Surface Functionalization of Titanium with Chitosan/Gelatin via Electrophoretic Deposition: Characterization and Cell Behavior. *Biomacromolecules* **2010**, *11* (5), 1254−1260.
(27) Ferraria, A. M.; Carapeto, A. P.; Botelho do Rego, A. M. X-ray Photoelectron Spectroscopy: Silver Salts Revisited. *Vacuum* **2012**, *86* (12), 1988−1991.
(28) Tjeng, L.; Meinders, M.; Van Elp, J.; Ghijsen, J.; Sawatzky, G.; Johnson, R. Electronic Structure of Ag 2 O. *Phys. Rev. B: Condens. Matter Mater. Phys.* **1990**, *41* (5), 3190.
(29) Kumari, P.; Majewski, P. Adsorption of Albumin on Silica Surfaces Modified by Silver and Copper Nanoparticles. *J. Nanomater.* **2013**, *2013*, 1.
(30) Chen, Q.; Shi, W.; Xu, Y.; Wu, D.; Sun, Y. Visible-light-responsive Ag−Si Codoped Anatase TiO2 Photocatalyst with Enhanced Thermal Stability. *Mater. Chem. Phys.* **2011**, *125* (3), 825−832.
(31) Wang, J.; Li, J.; Qian, S.; Guo, G.; Wang, Q.; Tang, J.; Shen, H.; Liu, X.; Zhang, X.; Chu, P. K. Antibacterial Surface Design of Titanium-Based Biomaterials for Enhanced Bacteria-Killing and Cell-Assisting Functions Against Periprosthetic Joint Infection. *ACS Appl. Mater. Interfaces* **2016**, *8* (17), 11162−11178.
(32) Gristina, A. Biomaterial-Centered Infection: Microbial Adhesion Versus Tissue Integration. *Science* **1987**, *237* (4822), 1588−1595.
(33) Smith, A. W. Biofilms and Antibiotic Therapy: Is there a Role for Combating Bacterial Resistance by the use of Novel Drug Delivery Systems? *Adv. Drug Delivery Rev.* **2005**, *57* (10), 1539−1550.
(34) AshaRani, P. V.; Low Kah Mun, G.; Hande, M. P.; Valiyaveettil, S. Cytotoxicity and Genotoxicity of Silver Nanoparticles in Human Cells. *ACS Nano* **2009**, *3* (2), 279−290.
(35) Patel, N.; Pai, M. P.; Rodvold, K. A.; Lomaestro, B.; Drusano, G. L.; Lodise, T. P. Vancomycin: We Can't Get There From Here. *Clin. Infect. Dis.* **2011**, *52* (8), 969−974.
(36) ISO, Iso 10993−5: Biological Evaluation of Medical Devices -- Part 5: Tests for In Vitro Cytotoxicity, 2009.
(37) Kumar-Krishnan, S.; Prokhorov, E.; Hernández-Iturriaga, M.; Mota-Morales, J. D.; Vázquez-Lepe, M.; Kovalenko, Y.; Sanchez, I. C.; Luna-Bárcenas, G. Chitosan/Silver Nanocomposites: Synergistic Antibacterial Action of Silver Nanoparticles and Silver Ions. *Eur. Polym. J.* **2015**, *67*, 242−251.
(38) Huang, L.; Dai, T.; Xuan, Y.; Tegos, G. P.; Hamblin, M. R. Synergistic Combination of Chitosan Acetate with Nanoparticle Silver as a Topical Antimicrobial: Efficacy against Bacterial Burn Infections. *Antimicrob. Agents Chemother.* **2011**, *55* (7), 3432−3438.
(39) Potara, M.; Jakab, E.; Damert, A.; Popescu, O.; Canpean, V.; Astilean, S. Synergistic Antibacterial Activity of Chitosan−Silver Nanocomposites on Staphylococcus aureus. *Nanotechnology* **2011**, *22* (13), 135101.
(40) Rai, M. K.; Deshmukh, S. D.; Ingle, A. P.; Gade, A. K. Silver Nanoparticles: the Powerful Nanoweapon Against Multidrug-Resistant Bacteria. *J. Appl. Microbiol.* **2012**, *112* (5), 841−852.
(41) Necula, B. S.; van Leeuwen, J. P. T. M.; Fratila-Apachitei, L. E.; Zaat, S. A. J.; Apachitei, I.; Duszczyk, J. In Vitro Cytotoxicity Evaluation of Porous TiO2−Ag Antibacterial Coatings for Human Fetal Osteoblasts. *Acta Biomater.* **2012**, *8* (11), 4191−4197.
(42) Xu, Z.; Li, M.; Li, X.; Liu, X.; Ma, F.; Wu, S.; Yeung, K. W. K.; Han, Y.; Chu, P. K. Antibacterial Activity of Silver Doped Titanate Nanowires on Ti Implants. *ACS Appl. Mater. Interfaces* **2016**, *8* (26), 16584−16594.
(43) Morones-Ramirez, J. R.; Winkler, J. A.; Spina, C. S.; Collins, J. J. Silver Enhances Antibiotic Activity Against Gram-Negative Bacteria. *Sci. Transl. Med.* **2013**, *5* (190), 190ra81−190ra81.
(44) Costerton, J. W.; Stewart, P. S.; Greenberg, E. P. Bacterial Biofilms: A Common Cause of Persistent Infections. *Science* **1999**, *284* (5418), 1318−1322.
(45) Sandoe, J. A. T.; Barlow, G.; Chambers, J. B.; Gammage, M.; Guleri, A.; Howard, P.; Olson, E.; Perry, J. D.; Prendergast, B. D.; Spry, M. J.; Steeds, R. P.; Tayebjee, M. H.; Watkin, R. Guidelines for the Diagnosis, Prevention and Management of Implantable Cardiac Electronic Device Infection. Report of A Joint Working Party Project on Behalf of the British Society for Antimicrobial Chemotherapy (Bsac, Host Organization), British Heart Rhythm Society (Bhrs), British Cardiovascular Society (Bcs), British Heart Valve Society (Bhvs) and British Society for Echocardiography (Bse). *J. Antimicrob. Chemother.* **2015**, *70* (2), 325−359.
(46) Gorgin Karaji, Z.; Speirs, M.; Dadbakhsh, S.; Kruth, J. P.; Weinans, H.; Zadpoor, A. A.; Amin Yavari, S. Additively Manufactured and Surface Biofunctionalized Porous Nitinol. *ACS Appl. Mater. Interfaces* **2017**, *9* (2), 1293−1304.
(47) van Leeuwen, B. L.; Kamps, W. A.; Jansen, H. W. B.; Hoekstra, H. J. The Effect of Chemotherapy on the Growing Skeleton. *Cancer Treat. Rev.* **2000**, *26* (5), 363−376.
(48) Davies, J. H.; Evans, B. A. J.; Jenney, M. E. M.; Gregory, J. W. In Vitro Effects of Combination Chemotherapy on Osteoblasts: Implications for Osteopenia in Childhood Malignancy. *Bone* **2002**, *31* (2), 319−326.
(49) Sala, A.; Barr, R. D. Osteopenia and Cancer in Children and Adolescents. *Cancer* **2007**, *109* (7), 1420−1431.

DOI: 10.1021/acsami.7b04950
ACS Appl. Mater. Interfaces 2017, 9, 25691−25699